



A CP violation measurement of B_s mesons at ATLAS and the LHC

Adam Barton
ATLAS Collaboration

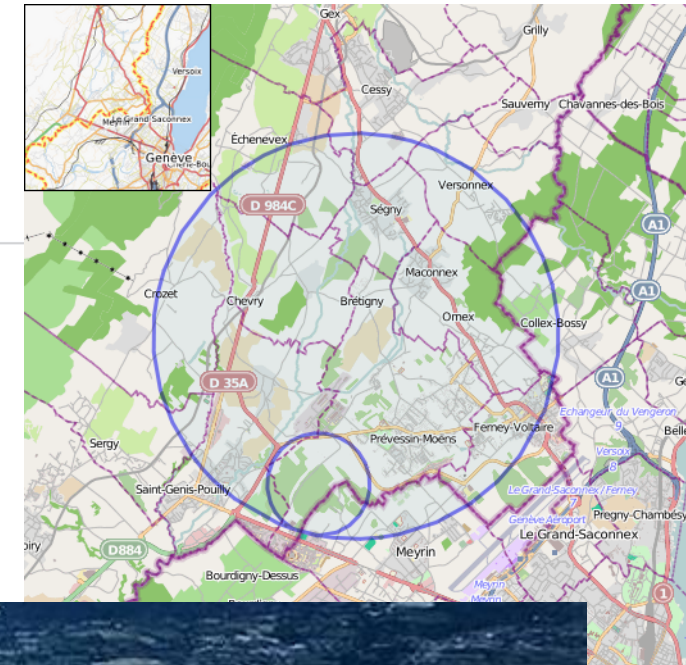
The LHC

The large hadron collider is the world's largest and highest energy synchrotron collider in the world.

It is built and run by CERN (the European/Everyone Organization for Nuclear Research)

It can collide protons at energies of 14 TeV, (currently running at 13TeV)

It is located in a 27 kilometer tunnel under Geneva near the Jura mountains.



The ATLAS (A Toroidal LHC ApparatuS) detector

ATLAS is a 45 by 50 metres in

Muon Spectrometer:

- (1) Monitored Drift Tube
- (2) Thin Gap Chamber

Magnet system:

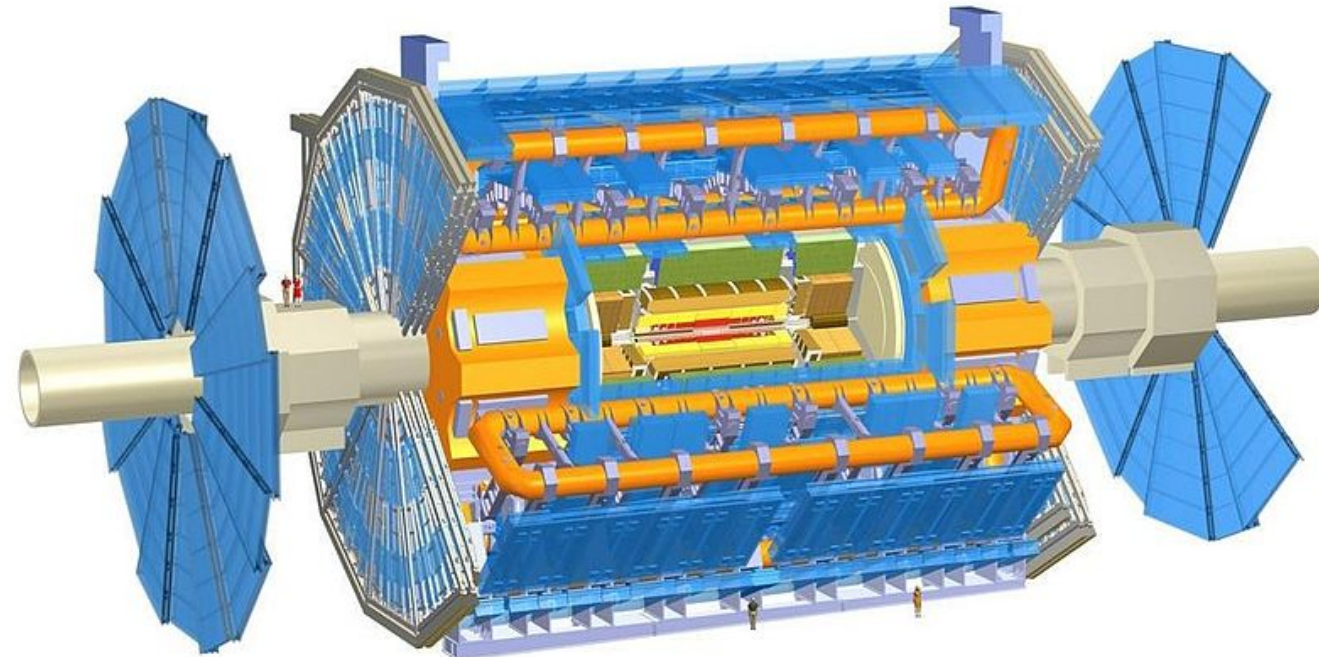
- (3) End-Cap Toroid Magnet
- (4) Barrel Toroid Magnet

Inner Detector:

- (5) Transition Radiation Tracker
- (6) Semi-Conductor Tracker
- (7) Pixel Detector

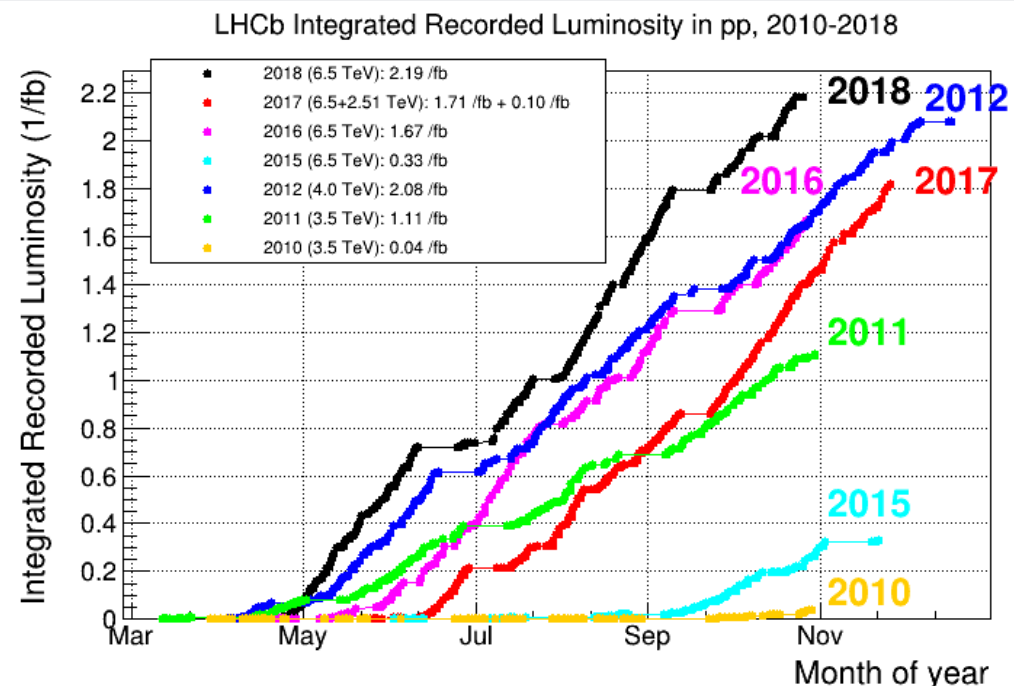
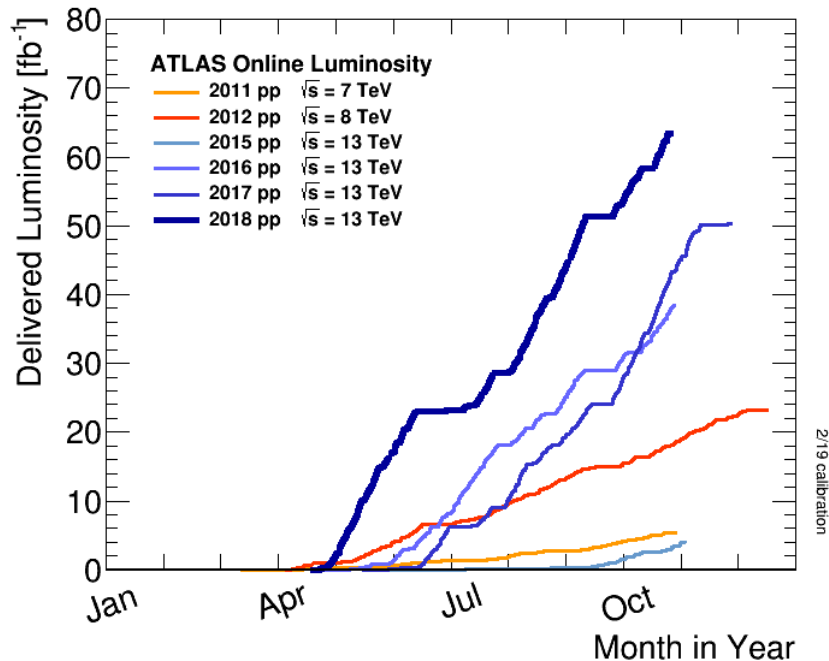
Calorimeters:

- (8) Electromagnetic Calorimeter
- (9) Hadronic Calorimeter



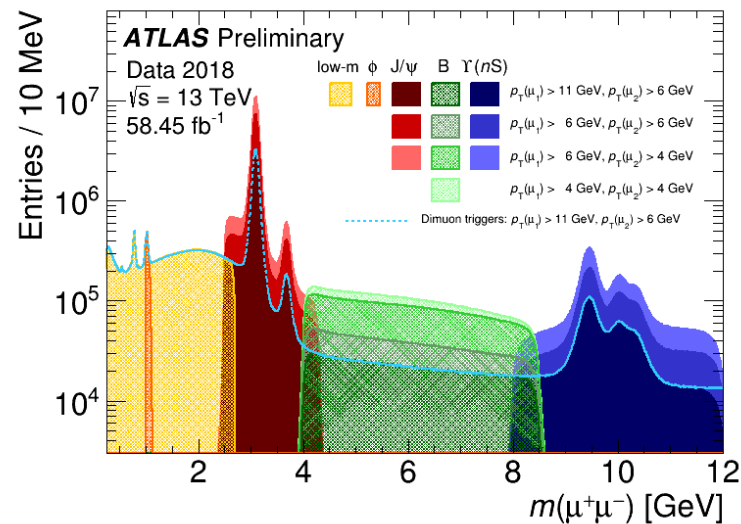
At the start of run 2 (2015) an insertable B-layer was installed to give better vertex and lifetime resolution

Data Collection



B-physics and Light-States

- ATLAS B-physics and Light-States programme:
 - Comprehensive measurements across a variety of decay modes:
 - Precise property measurements including CPV ($B_s \rightarrow J/\psi \phi$)
 - Cross-section measurements including Quarkonium
 - Rare decay processes; e.g FCNC $B_{(s,d)} \rightarrow \mu\mu$
 - Spectroscopy, exotic states (e.g pentaquarks)
 - Charged lepton flavour violation ($\tau \rightarrow 3\mu$)
- Typically rely on low-pT di-muon signatures.



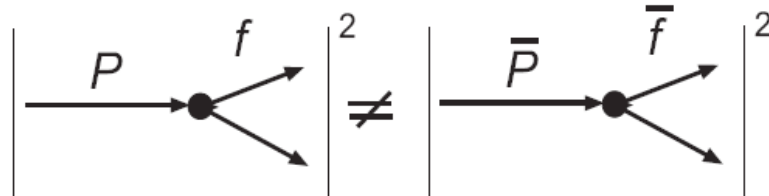


Introduction to the CP violation

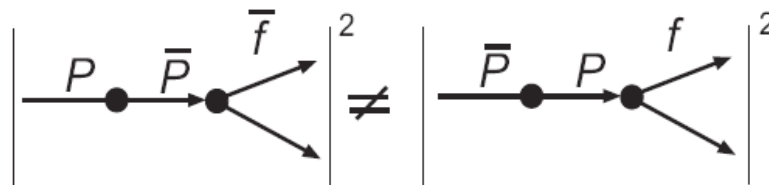
- Charge Parity (CP) symmetries mean that particle interactions should produce matter and antimatter in equal quantities
- In 1967 Soviet Nuclear Physicist Andrei Sakharov proposed CP violation:
 - Since the observed universe seems devoid of stable antimatter there must be baryon number violating transitions in particle physics.
 - CP has to be violated otherwise there would be equal amounts of anti matter
 - CP violations must occur during interactions and not in thermal equilibrium



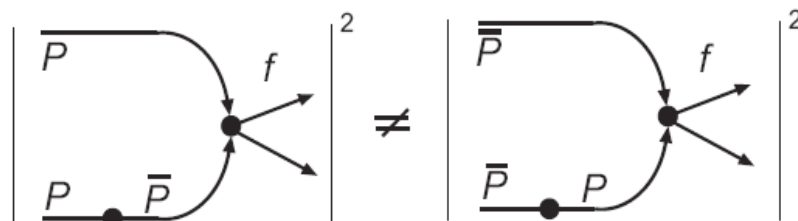
3 Types of CP violation



(a) Direct CP violation.



(b) CP violation in mixing.



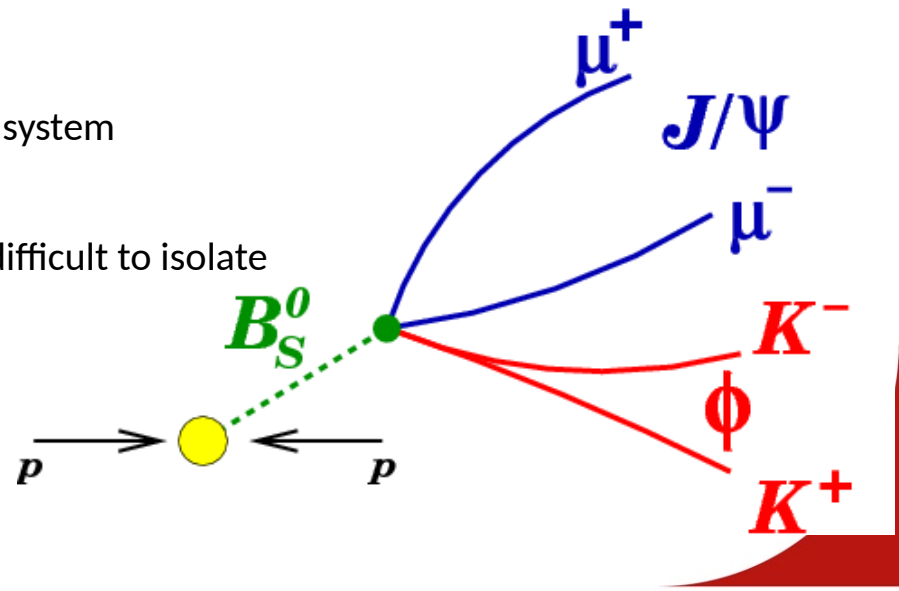
(c) CP violation in interference.

Exclusive decay chain

- While φ_s can be accessed a number of ways the easiest way at ATLAS is through the exclusive decay $B_s \rightarrow J/\Psi \phi$ where

- $J/\Psi \rightarrow \mu^+ \mu^-$ selected nicely from the muon system

- $\phi \rightarrow K^+ K^-$ ATLAS has no particle ID so this is difficult to isolate



CP Violation in neutral B_s system

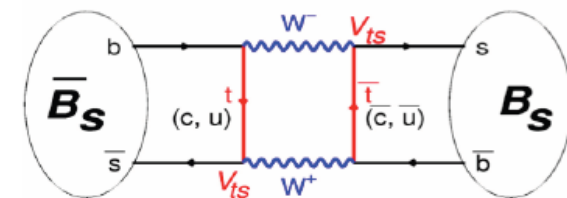
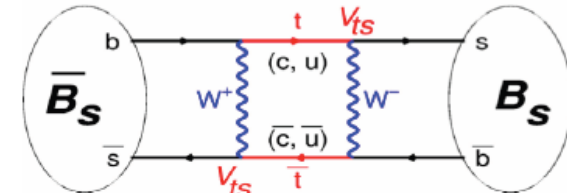
Mixing of flavour eigenstates are governed by:

$$i \frac{d}{dt} \begin{pmatrix} B_s^0(t) \\ \bar{B}_s^0(t) \end{pmatrix} = H \begin{pmatrix} B_s^0(t) \\ \bar{B}_s^0(t) \end{pmatrix} \equiv \left[\underbrace{\begin{pmatrix} M_0 & M_{12} \\ M_{12}^* & M_0 \end{pmatrix}}_{\text{mass matrix}} - \underbrace{\frac{i}{2} \begin{pmatrix} \Gamma_0 & \Gamma_{12} \\ \Gamma_{12}^* & \Gamma_0 \end{pmatrix}}_{\text{decay matrix}} \right] \begin{pmatrix} B_s^0(t) \\ \bar{B}_s^0(t) \end{pmatrix}$$

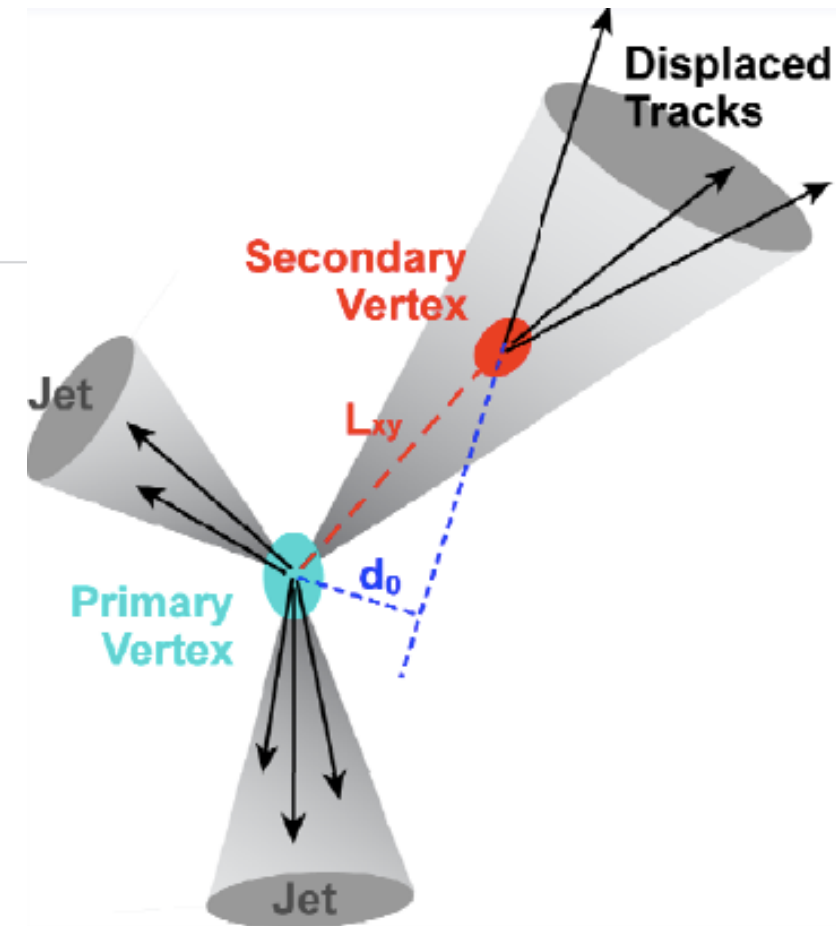
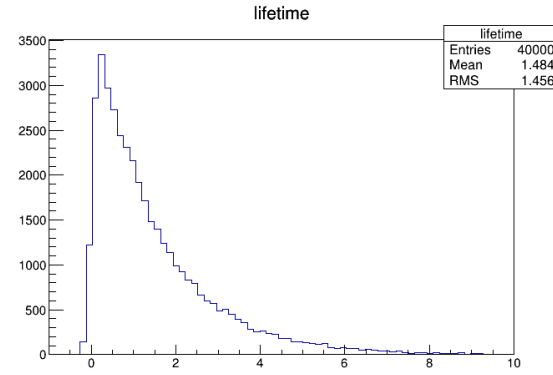
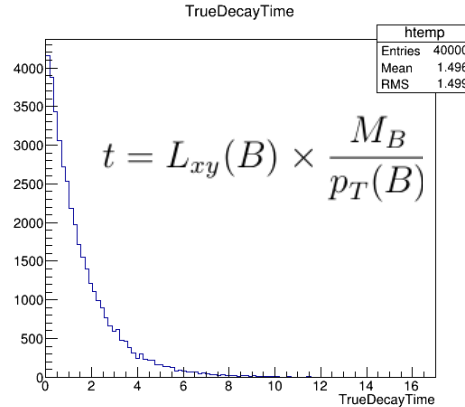
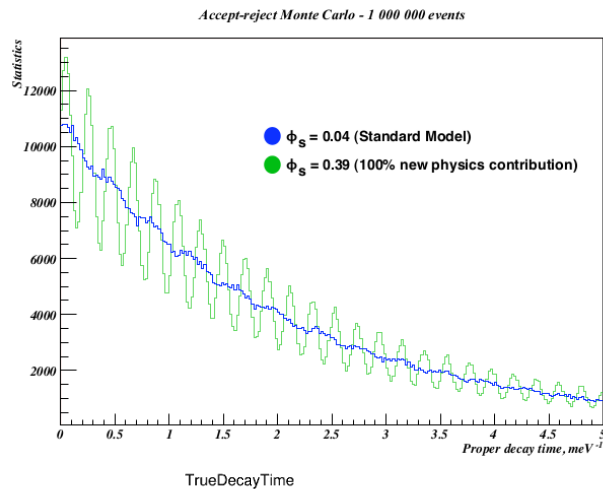
- The mass eigenstates

$$\begin{aligned} |B_s^H\rangle &= p |B_s^0\rangle - q |\bar{B}_s^0\rangle \\ |B_s^L\rangle &= p |B_s^0\rangle + q |\bar{B}_s^0\rangle \end{aligned}$$

- $\Delta m_s = m_H - m_L \approx 2|M_{12}|$
- $\varphi_s^{\text{SM}} = \arg(-M_{12}/\Gamma_{12}) \approx -0.04$ - CP violating phase
- Γ is the average lifetime of the two states $(\Gamma_L + \Gamma_H)/2$
- $\Delta\Gamma = \Gamma_L - \Gamma_H \approx 2 |\Gamma_{12}| \cos(2 \varphi_s^{\text{SM}})$ – Can be considered the difference of the two lifetime states



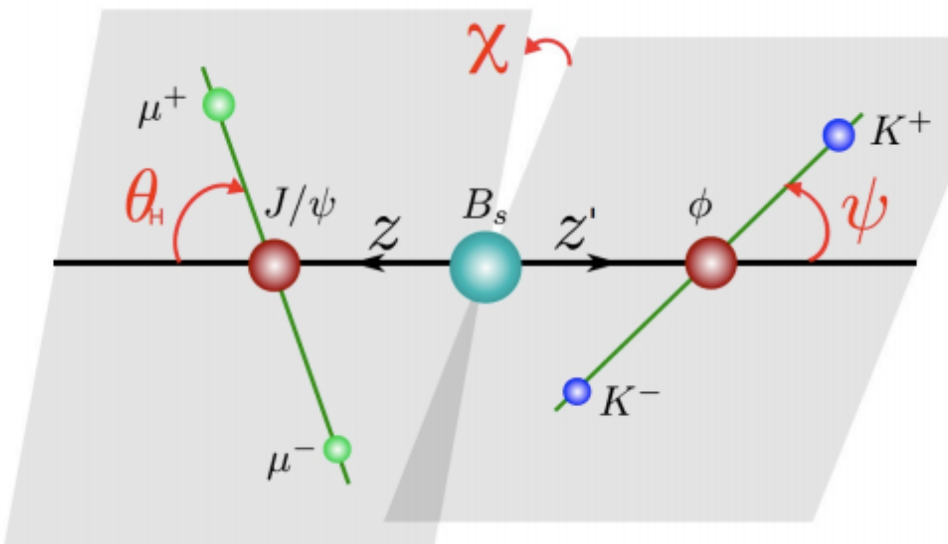
Measuring a particle lifetime



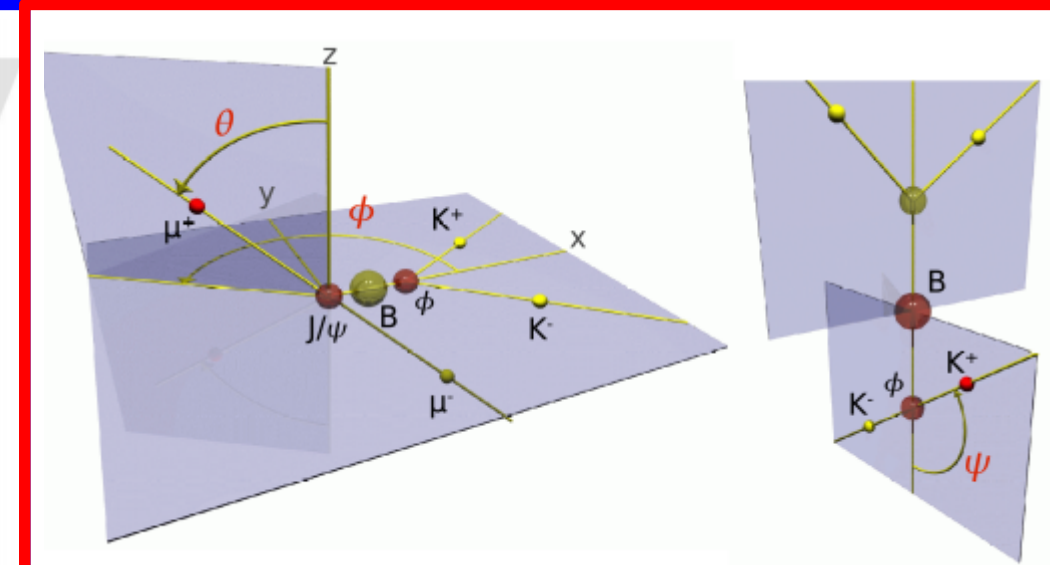
Angular Systems for $B_s \rightarrow J/\psi \phi$

- You can access the key physical variables for this decay using one of 2 angular definitions

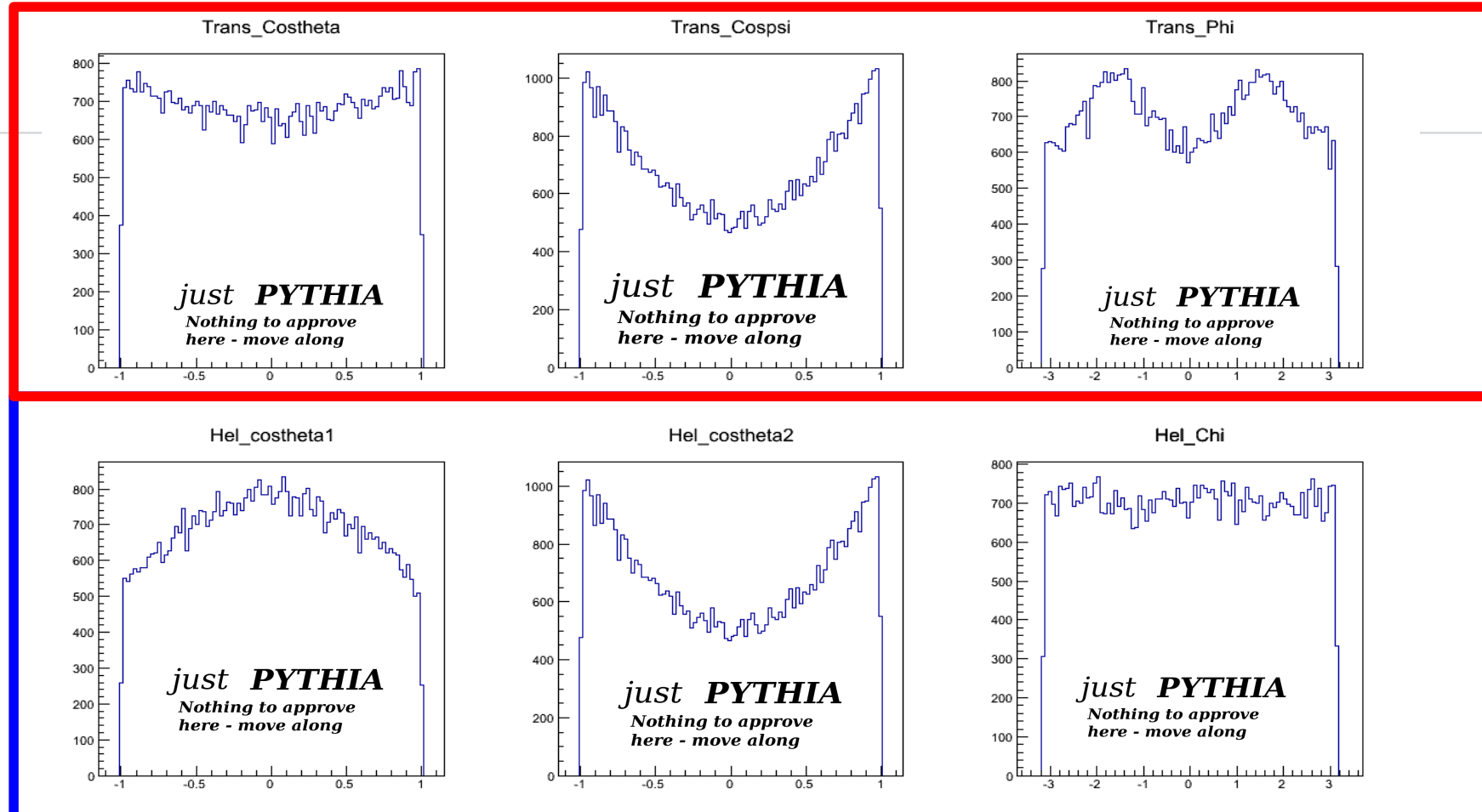
Helicity Basis



Transversity Basis



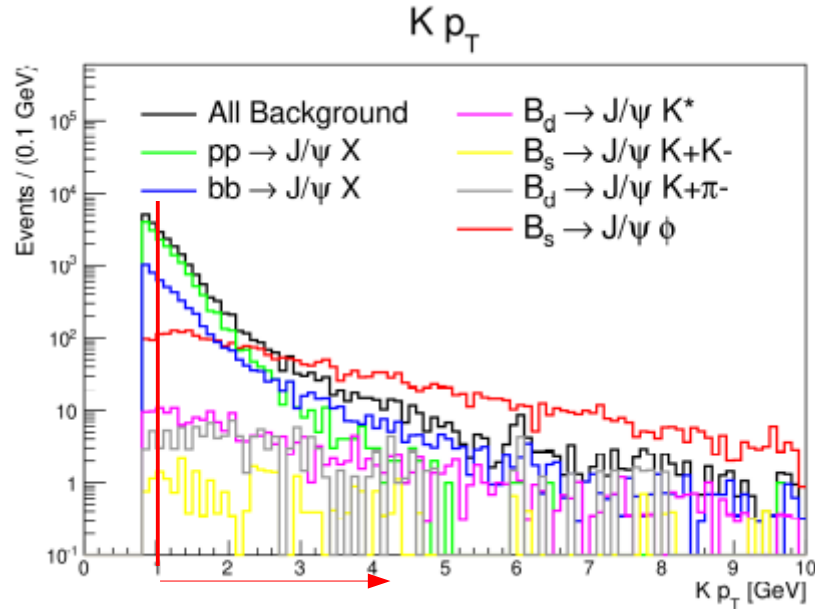
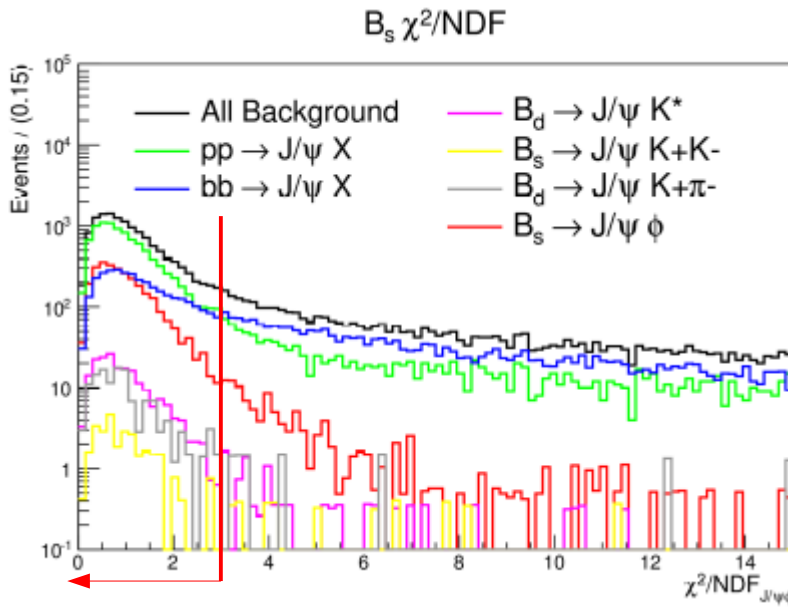
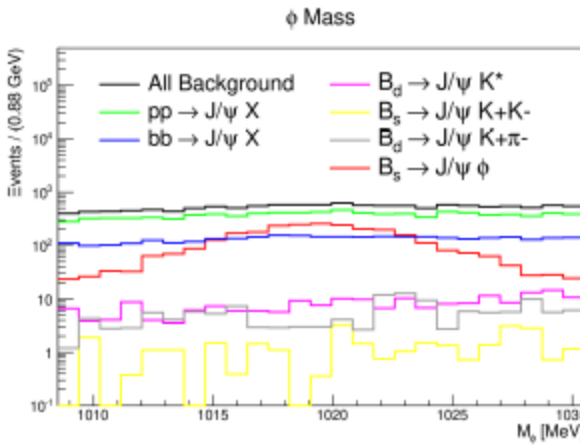
What the signal looks like



ATLAS Publications

- Time dependent untagged ϕ_s and $\Delta\Gamma_s$ from $B_s \rightarrow J/\psi\phi$ JHEP 1212 (2012) 072 - 02-AUG-12
- Time dependent flavour-tagged ϕ_s and $\Delta\Gamma_s$ from $B_s \rightarrow J/\psi\phi$ at 7 TeV Phys. Rev. D. 90, 052007 (2014) 05-JUL-14
- Time dependent flavour-tagged ϕ_s and $\Delta\Gamma_s$ from $B_s \rightarrow J/\psi\phi$ in Run 1 JHEP 08 (2016) 147 13-JAN-16
- Measurement of the CP violation phase ϕ_s in $B_s \rightarrow J/\psi\phi$ decays in ATLAS at 13 TeV 23 Mar 2019 (Conf-Note going to publication)
- Next paper will include all Run-2 data.

Deciding cuts





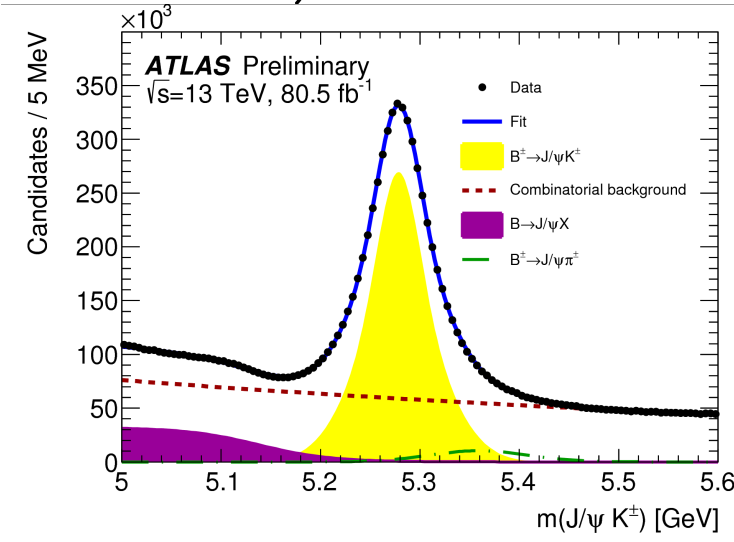
Deciding Cuts

ATLAS-CONF-2019-009

- This analysis follows a previous measurement using 19.2 fb^{-1} of $\sqrt{s}=7 \text{ TeV}$ and 8 TeV ("run 1")
- The new analysis uses datasets from 2015 to 2017 with $\sqrt{s}=13 \text{ TeV}$ totalling 80.5 fb^{-1} .
- Full decay reconstruction using inner detector and muon detectors, no K/pi separation:
 - J/ψ selection – di-muon vertex $\chi^2/\text{NDF} < 10$, J/ψ invariant mass windows width $0.27 \dots 0.48 \text{ GeV}$ (barrel \rightarrow endcap)
 - ϕ selection – $p_T(K^\pm) > 1 \text{ GeV}$, Invariant mass window 22 MeV
 - B candidates – 4-track vertex $\chi^2/\text{NDF} < 3$, $(5.15 - 5.65) \text{ GeV}$, no proper decay time cut.

Flavour Tagging

- The analysis gains precision with tagging information. We use opposite-side tagging (OST).
- We use 4 tagging methods: “Tight” muons, electrons, Low- p_T muons, Jet
- Charge of p_T -weighted tracks in a cone around the opposite primary object, used to build per-candidate B_s tag probability.
- Calibrated from $B^+ \rightarrow J/\psi K^+$ sample

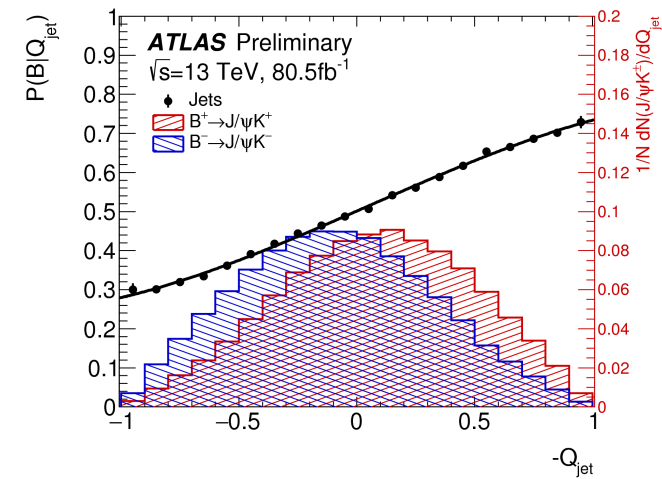
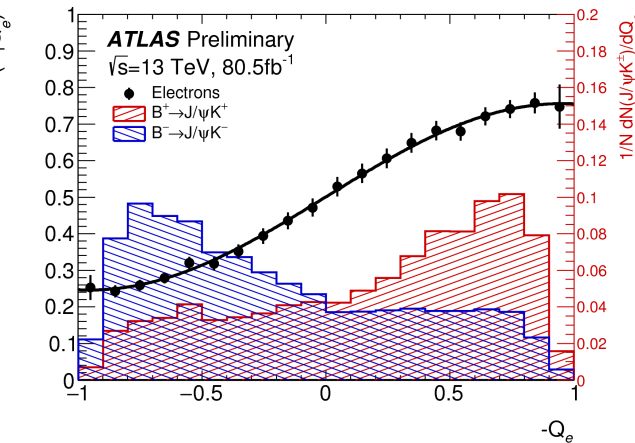
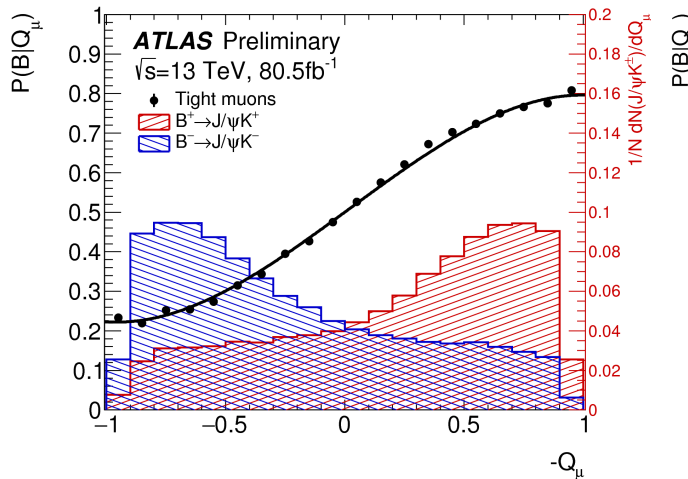


Tagging: weighted sum of charge in a cone

$$Q_x = \frac{\sum_i^N \text{tracks} q_i \cdot (p_{Ti})^\kappa}{\sum_i^N \text{tracks} (p_{Ti})^\kappa},$$

| Tag method | Efficiency [%] | Effective Dilution [%] | Tagging Power [%] |
|-----------------|------------------|------------------------|-------------------|
| Tight muon | 4.50 ± 0.01 | 43.8 ± 0.2 | 0.862 ± 0.009 |
| Electron | 1.57 ± 0.01 | 41.8 ± 0.2 | 0.274 ± 0.004 |
| Low- p_T muon | 3.12 ± 0.01 | 29.9 ± 0.2 | 0.278 ± 0.006 |
| Jet | 5.54 ± 0.01 | 20.4 ± 0.1 | 0.231 ± 0.005 |
| Total | 14.74 ± 0.02 | 33.4 ± 0.1 | 1.65 ± 0.01 |

In events where multiple methods are available the highest dilution is selected.



Symmetries: $\{\phi_s, \Delta\Gamma_s, \delta_{\perp}, \delta_{\parallel}\} \rightarrow \{\pi - \phi_s, -\Delta\Gamma_s, \pi - \delta_{\perp}, 2\pi - \delta_{\parallel}\}$

~~$\{\phi_s, \Delta\Gamma_s, \delta_{\perp}, \delta_{\parallel}, \delta_S\} \rightarrow \{-\phi_s, \Delta\Gamma_s, \pi - \delta_{\perp}, -\delta_{\parallel}, -\delta_S\}$~~ (untagged fit only)

Signal Likelihood

| k | $O^{(k)}(t)$ | $g^{(k)}(\theta_T, \psi_T, \phi_T)$ |
|-----|--|--|
| 1 | $\frac{1}{2} A_0(0) ^2 \left[(1 + \cos \phi_s) e^{-\Gamma_L^{(s)} t} + (1 - \cos \phi_s) e^{-\Gamma_H^{(s)} t} \pm 2e^{-\Gamma_s t} \sin(\Delta m_s t) \sin \phi_s \right]$ | $2 \cos^2 \psi_T (1 - \sin^2 \theta_T \cos^2 \phi_T)$ |
| 2 | $\frac{1}{2} A_{\parallel}(0) ^2 \left[(1 + \cos \phi_s) e^{-\Gamma_L^{(s)} t} + (1 - \cos \phi_s) e^{-\Gamma_H^{(s)} t} \pm 2e^{-\Gamma_s t} \sin(\Delta m_s t) \sin \phi_s \right]$ | $\sin^2 \psi_T (1 - \sin^2 \theta_T \sin^2 \phi_T)$ |
| 3 | $\frac{1}{2} A_{\perp}(0) ^2 \left[(1 - \cos \phi_s) e^{-\Gamma_L^{(s)} t} + (1 + \cos \phi_s) e^{-\Gamma_H^{(s)} t} \mp 2e^{-\Gamma_s t} \sin(\Delta m_s t) \sin \phi_s \right]$ | $\sin^2 \psi_T \sin^2 \theta_T$ |
| 4 | $\frac{1}{2} A_0(0) A_{\parallel}(0) \cos \delta_{\parallel}$ $\left[(1 + \cos \phi_s) e^{-\Gamma_L^{(s)} t} + (1 - \cos \phi_s) e^{-\Gamma_H^{(s)} t} \pm 2e^{-\Gamma_s t} \sin(\Delta m_s t) \sin \phi_s \right]$ | $\frac{1}{\sqrt{2}} \sin 2\psi_T \sin^2 \theta_T \sin 2\phi_T$ |
| 5 | $ A_{\parallel}(0) A_{\perp}(0) \left[\frac{1}{2}(e^{-\Gamma_L^{(s)} t} - e^{-\Gamma_H^{(s)} t}) \cos(\delta_{\perp} - \delta_{\parallel}) \sin \phi_s \right.$ $\left. \pm e^{-\Gamma_s t} (\sin(\delta_{\perp} - \delta_{\parallel}) \cos(\Delta m_s t) - \cos(\delta_{\perp} - \delta_{\parallel}) \cos \phi_s \sin(\Delta m_s t)) \right]$ | $-\sin^2 \psi_T \sin 2\theta_T \sin \phi_T$ |
| 6 | $ A_0(0) A_{\perp}(0) \left[\frac{1}{2}(e^{-\Gamma_L^{(s)} t} - e^{-\Gamma_H^{(s)} t}) \cos \delta_{\perp} \sin \phi_s \right.$ $\left. \pm e^{-\Gamma_s t} (\sin \delta_{\perp} \cos(\Delta m_s t) - \cos \delta_{\perp} \cos \phi_s \sin(\Delta m_s t)) \right]$ | $\frac{1}{\sqrt{2}} \sin 2\psi_T \sin 2\theta_T \cos \phi_T$ |
| 7 | $\frac{1}{2} A_S(0) ^2 \left[(1 - \cos \phi_s) e^{-\Gamma_L^{(s)} t} + (1 + \cos \phi_s) e^{-\Gamma_H^{(s)} t} \mp 2e^{-\Gamma_s t} \sin(\Delta m_s t) \sin \phi_s \right]$ | $\frac{2}{3} (1 - \sin^2 \theta_T \cos^2 \phi_T)$ |
| 8 | $\alpha A_S(0) A_{\parallel}(0) \left[\frac{1}{2}(e^{-\Gamma_L^{(s)} t} - e^{-\Gamma_H^{(s)} t}) \sin(\delta_{\parallel} - \delta_S) \sin \phi_s \right.$ $\left. \pm e^{-\Gamma_s t} (\cos(\delta_{\parallel} - \delta_S) \cos(\Delta m_s t) - \sin(\delta_{\parallel} - \delta_S) \cos \phi_s \sin(\Delta m_s t)) \right]$ | $\frac{1}{3} \sqrt{6} \sin \psi_T \sin^2 \theta_T \sin 2\phi_T$ |
| 9 | $\frac{1}{2}\alpha A_S(0) A_{\perp}(0) \sin(\delta_{\perp} - \delta_S)$ $\left[(1 - \cos \phi_s) e^{-\Gamma_L^{(s)} t} + (1 + \cos \phi_s) e^{-\Gamma_H^{(s)} t} \mp 2e^{-\Gamma_s t} \sin(\Delta m_s t) \sin \phi_s \right]$ | $\frac{1}{3} \sqrt{6} \sin \psi_T \sin 2\theta_T \cos \phi_T$ |
| 10 | $\alpha A_0(0) A_S(0) \left[\frac{1}{2}(e^{-\Gamma_H^{(s)} t} - e^{-\Gamma_L^{(s)} t}) \sin \delta_S \sin \phi_s \right.$ $\left. \pm e^{-\Gamma_s t} (\cos \delta_S \cos(\Delta m_s t) + \sin \delta_S \cos \phi_s \sin(\Delta m_s t)) \right]$ | $\frac{4}{3} \sqrt{3} \cos \psi_T (1 - \sin^2 \theta_T \cos^2 \phi_T)$ |

CP +1
CP +1
CP -1

Interference terms

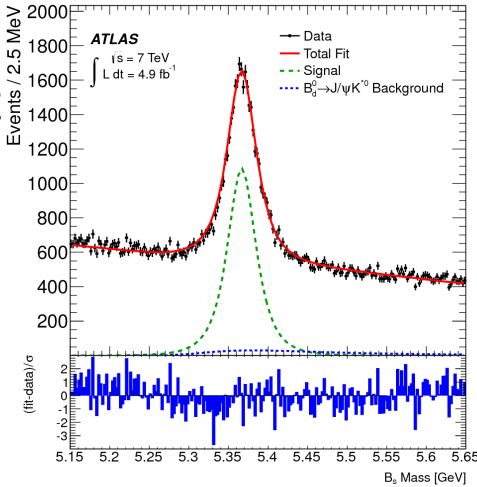
S-wave terms

The solution with a negative $\Delta\Gamma_s$ is excluded using another LHCb measurement which determines the $\Delta\Gamma_s$ to be positive

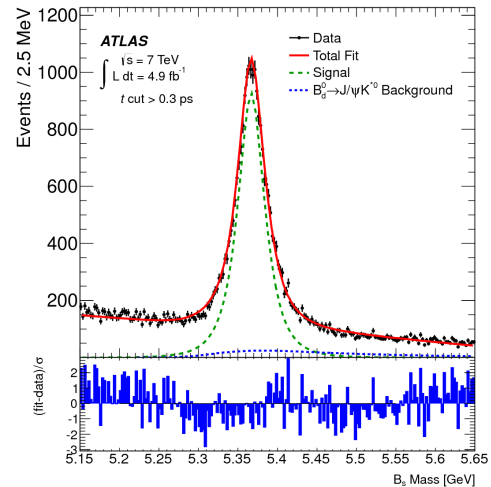
Background description

- To make a precision measurement it is necessary to either exclude or accurately describe the background
- The different backgrounds present are:
- Direct $pp \rightarrow J/\psi$ background
- Misreconstructed complete decays such as $B_d \rightarrow J/\psi K^*$ and $\Lambda_b \rightarrow J/\psi \Lambda^*(Kp)$
- Miscellaneous combinatorics from $bb \rightarrow J/\psi X$

Mass spectrum including Direct background



Mass spectrum excluding direct background by lifetime cut



Unbinned Maximum Likelihood Fit

$$\ln \mathcal{L} = \sum_{i=1}^N \left[w_i \cdot \ln(f_s \cdot \mathcal{F}_s(m_i, t_i, \sigma_{t_i}, \Omega_i, P(B|Q), p_{T_i})) \right.$$

$$+ f_{B^0} \cdot \mathcal{F}_{B^0}(m_i, t_i, \sigma_{t_i}, \Omega_i, P(B|Q), p_{T_i})$$

$$+ f_{\Lambda_b} \cdot \mathcal{F}_{\Lambda_b}(m_i, t_i, \sigma_{t_i}, \Omega_i, P(B|Q), p_{T_i})$$

$$\left. + (1 - f_s \cdot (1 + f_{B^0} + f_{\Lambda_b})) \mathcal{F}_{\text{bkg}}(m_i, t_i, \sigma_{t_i}, \Omega_i, P(B|Q), p_{T_i})) \right\}$$

Measured variables:

B_s mass m_i

B_s proper decay time t_i
and its uncertainty σ_{t_i}

3 angles $\Omega_i(\theta_T, \psi_T, \phi_T)$

B_s momentum p_T

B_s tag probability $p_{B|Q_i}$
tagging method M_i

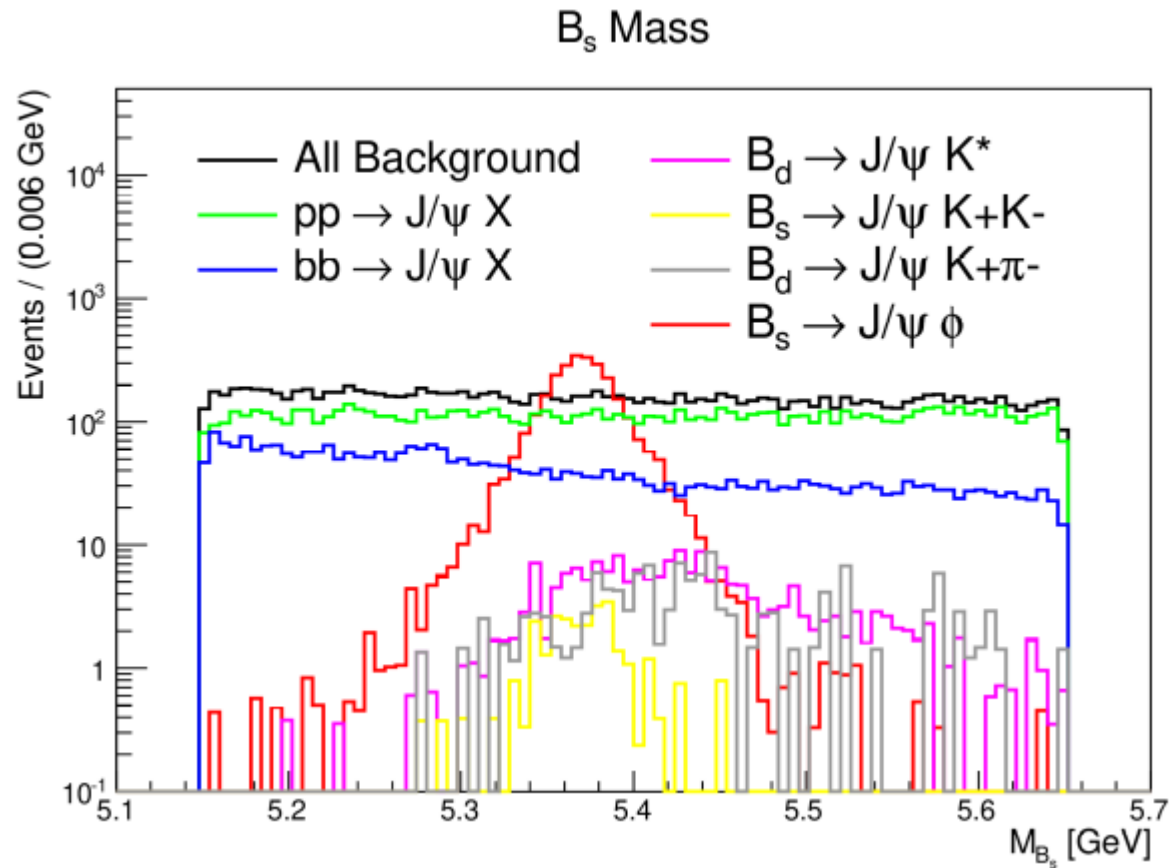
$B_d \rightarrow J/\psi K^*(K\pi)$ and $\Lambda_b \rightarrow J/\psi \Lambda^*(Kp)$ decay

reflections, derived from MC, PDG and the LHCb $\Lambda_b \rightarrow J/\psi Kp$ measurement; fixed shape and relative contribution in the fit

Combinatorial background description, derived from data sidebands; angular distribution described by spherical harmonics and fixed in the fit

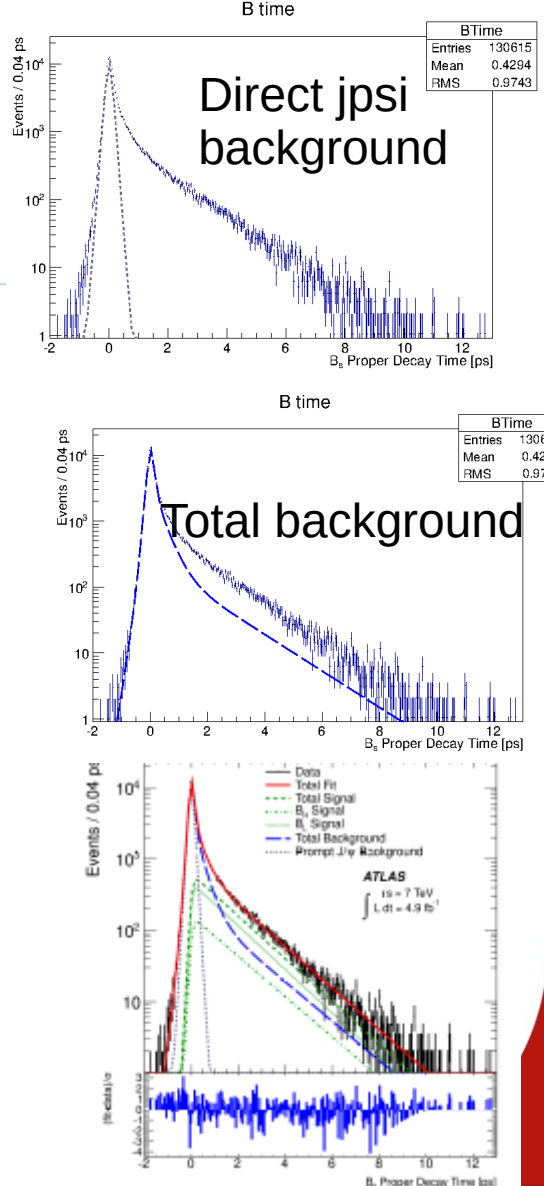
Weights accounting for **proper decay time trigger efficiency** (muons track d_0 reconstruction efficiency bias); estimated from MC

Background with Monte Carlo



Background representation in the fit

- Time component of background:
 - Prompt background: delta function at 0, convoluted by Gauss **per-candidate resolution** σ_{ti}
 - Two exponentials representing longer-lived backgrounds
 - Small negative exponential component for events with poor vertex resolution
- Background angular shapes
 - Arise from detector and kinematic sculpting
 - Described by empirical functions with parameters determined in the fit
- Background mass model – linear function
- $B^0 \rightarrow J/\psi K^{*0}$ and $\Lambda b \rightarrow J/\psi \Lambda^*(Kp)$ contamination treated separately
 - fractions are determined from MC
 - mass, angular shapes - from MC
 - used in PDF but no free parameters of fit



Angular Background

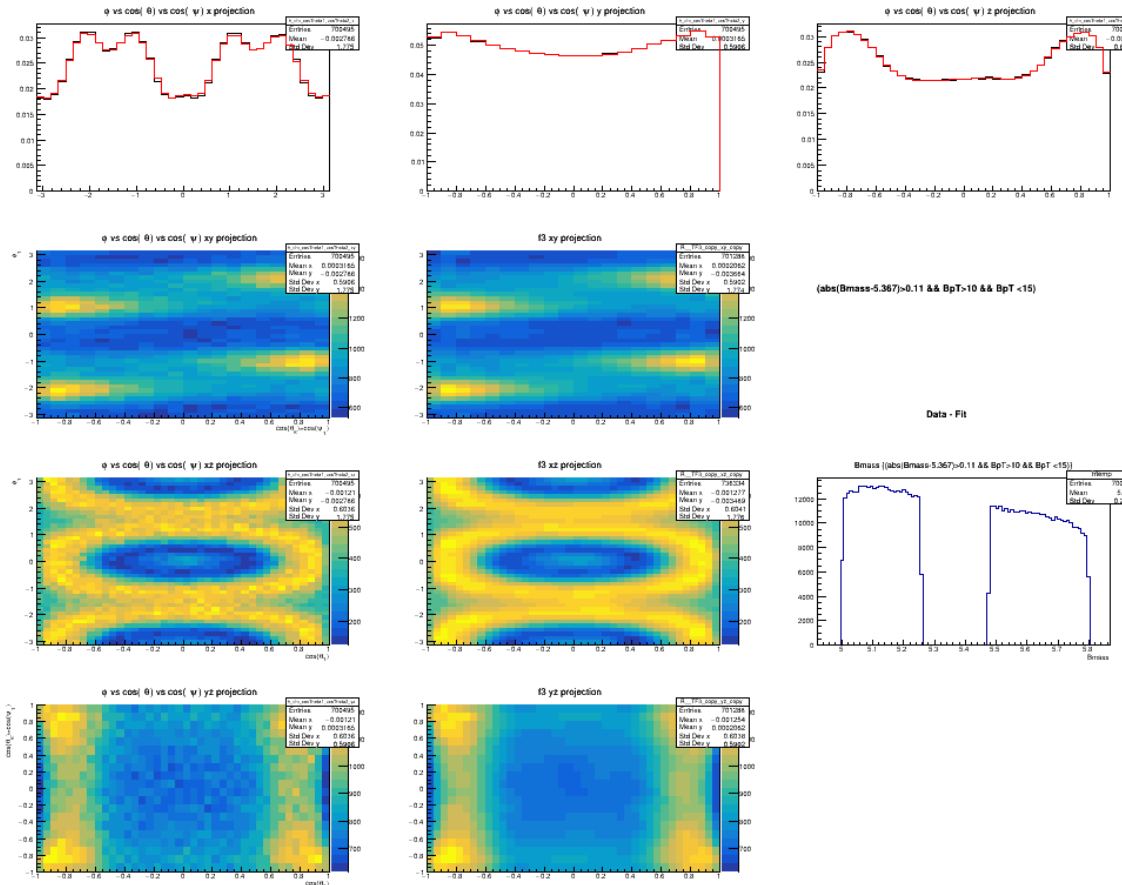
- The angular component of the background is shaped by detector and acceptance effects producing a non-trivial 3D shape that is also pT dependent
- The mass side bands are taken and a Legendre polynomial function is used to fit the shape. The resulting parameters are fixed and used in the main fit.
- The dedicated backgrounds are simulated with monte carlo, their shaping applied and also fit by spherical harmonics

$$Y_l^m(\theta_T) = \sqrt{(2l+1)/(4\pi)} \sqrt{(l-m)!/(l+m)!} P_l^{|m|}(\cos \theta_T)$$

$$P_k(x) = \frac{1}{2^k k!} \frac{d^k}{dx^k} (x^2 - 1)^k$$

$$\mathcal{P}_b(\theta_T, \psi_T, \phi_T) = \sum_{k=0}^{14} \sum_{l=0}^{14} \sum_{m=-l}^l \begin{cases} a_{k,l,m} \sqrt{2} Y_l^m(\theta_T) \cos(m\phi_T) P_k(\cos \psi_T) & \text{where } m > 0 \\ a_{k,l,m} \sqrt{2} Y_l^{-m}(\theta_T) \sin(m\phi_T) P_k(\cos \psi_T) & \text{where } m < 0 \\ a_{k,l,m} \sqrt{2} Y_l^0(\theta_T) P_k(\cos \psi_T) & \text{where } m = 0 \end{cases}$$

Angular Background

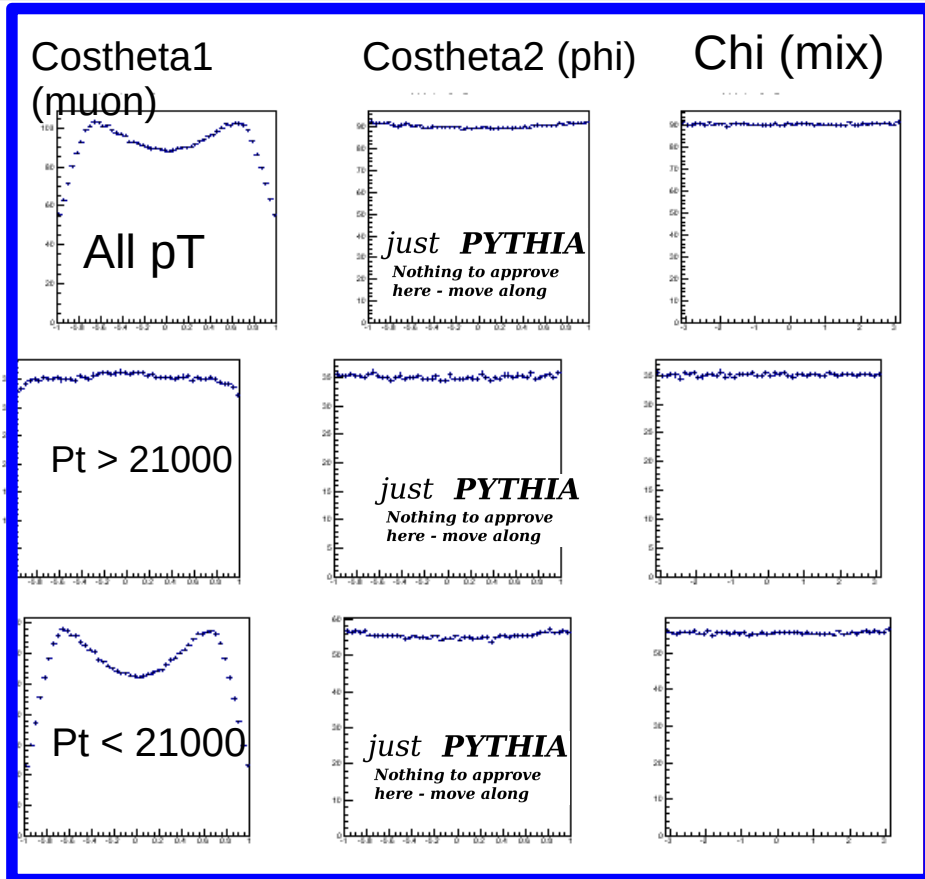


Kinematic Acceptance

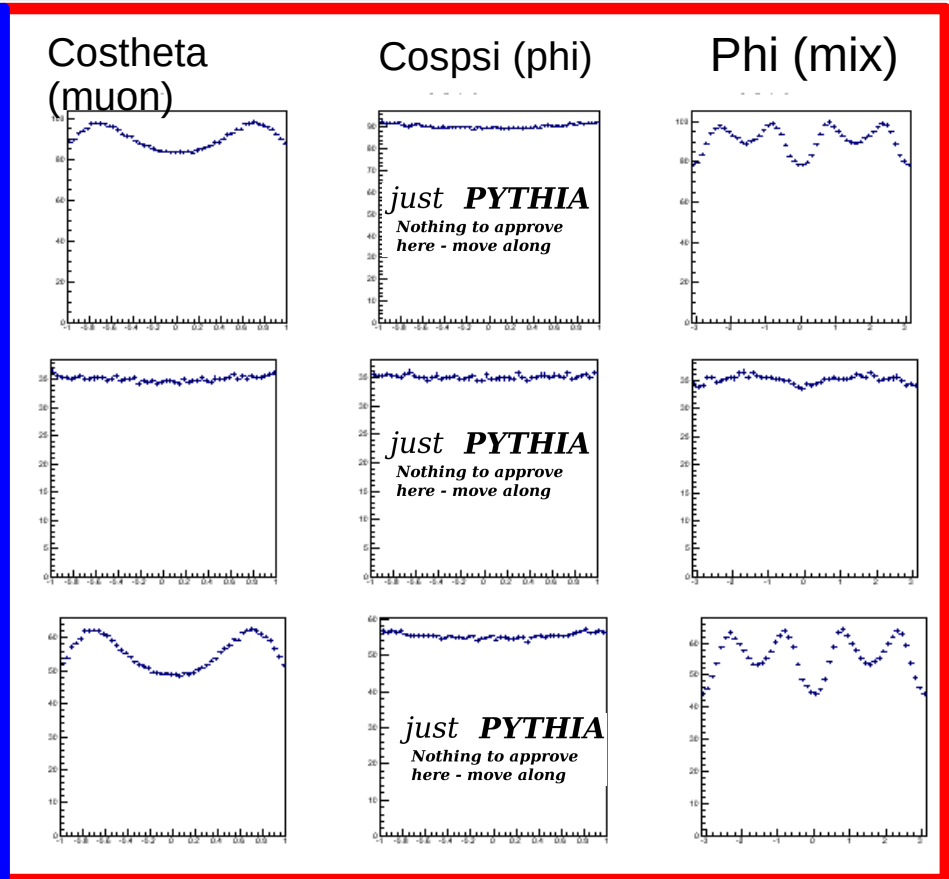
- It is necessary to exclude (cut) low energy tracks to exclude large quantities of background.
 - The muon trigger applies at least a 4GeV cut on the muons (triggers vary according to the luminosity)
 - Kaon cuts are applied after reconstruction to reduce the background.
- This biases the angular distributions distorting the “true” distribution.
- This is attained by simulating a naïve level of physics so the angular distributions are flat, and then feeding these events through the detector simulator and applying the standard cuts.

What Acceptances look like (mu4mu4)

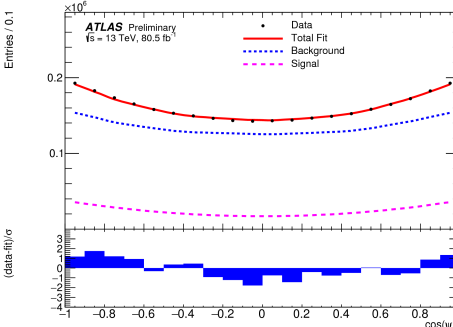
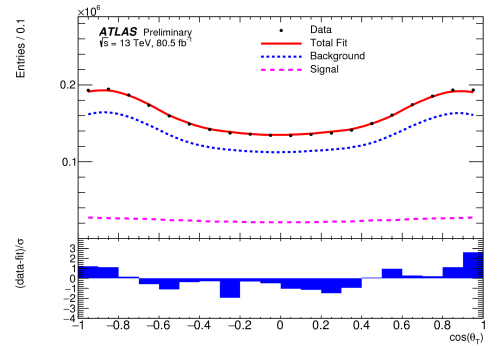
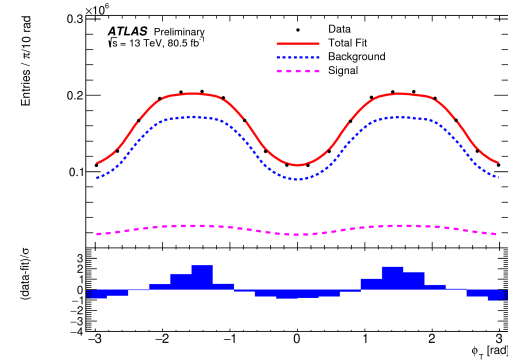
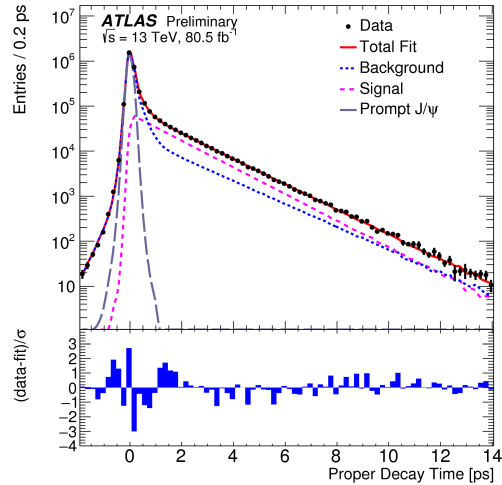
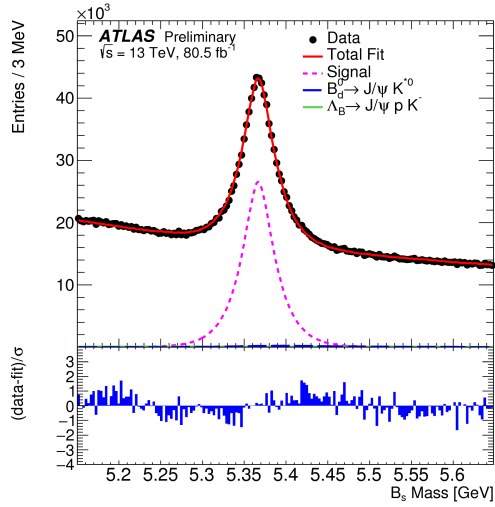
Helicity



Transversity



Fit Projections



Systematic Uncertainties

| | ϕ_s [rad] | $\Delta\Gamma_s$ [ps $^{-1}$] | Γ_s [ps $^{-1}$] | $ A_{ }(0) ^2$ | $ A_0(0) ^2$ | $ A_S(0) ^2$ | δ_\perp [rad] | $\delta_{ }$ [rad] | $\delta_\perp - \delta_S$ [rad] |
|--------------------------|----------------------|-----------------------------------|-----------------------------|----------------------|----------------------|----------------------|-------------------------|------------------------|------------------------------------|
| Tagging | 1.7×10^{-2} | 0.4×10^{-3} | 0.3×10^{-3} | 0.2×10^{-3} | 0.2×10^{-3} | 2.3×10^{-3} | 1.9×10^{-2} | 2.2×10^{-2} | 2.2×10^{-3} |
| Acceptance | 0.7×10^{-3} | $< 10^{-4}$ | $< 10^{-4}$ | 0.8×10^{-3} | 0.7×10^{-3} | 2.4×10^{-3} | 3.3×10^{-2} | 1.4×10^{-2} | 2.6×10^{-3} |
| ID alignment | 0.7×10^{-3} | 0.1×10^{-3} | 0.5×10^{-3} | $< 10^{-4}$ | $< 10^{-4}$ | $< 10^{-4}$ | 1.0×10^{-2} | 7.2×10^{-3} | $< 10^{-4}$ |
| S -wave phase | 0.2×10^{-3} | $< 10^{-4}$ | $< 10^{-4}$ | 0.3×10^{-3} | $< 10^{-4}$ | 0.3×10^{-3} | 1.1×10^{-2} | 2.1×10^{-2} | 8.3×10^{-3} |
| Background angles model: | | | | | | | | | |
| Choice of fit function | 1.8×10^{-3} | 0.8×10^{-3} | $< 10^{-4}$ | 1.4×10^{-3} | 0.7×10^{-3} | 0.2×10^{-3} | 8.5×10^{-2} | 1.9×10^{-1} | 1.8×10^{-3} |
| Choice of p_T bins | 1.3×10^{-3} | 0.5×10^{-3} | $< 10^{-4}$ | 0.4×10^{-3} | 0.5×10^{-3} | 1.2×10^{-3} | 1.5×10^{-3} | 7.2×10^{-3} | 1.0×10^{-3} |
| Choice of mass interval | 0.4×10^{-3} | 0.1×10^{-3} | 0.3×10^{-3} | 0.3×10^{-3} | 0.3×10^{-3} | 1.3×10^{-3} | 4.4×10^{-3} | 7.4×10^{-3} | 2.3×10^{-3} |
| Dedicated backgrounds: | | | | | | | | | |
| B_d^0 | 2.3×10^{-3} | 1.1×10^{-3} | $< 10^{-4}$ | 0.2×10^{-3} | 3.1×10^{-3} | 1.4×10^{-3} | 1.0×10^{-2} | 2.3×10^{-2} | 2.1×10^{-3} |
| Λ_b | 1.6×10^{-3} | 0.4×10^{-3} | 0.2×10^{-3} | 0.5×10^{-3} | 1.2×10^{-3} | 1.8×10^{-3} | 1.4×10^{-2} | 2.9×10^{-2} | 0.8×10^{-3} |
| Fit model: | | | | | | | | | |
| Time res. sig frac | 1.4×10^{-3} | 1.1×10^{-3} | $< 10^{-4}$ | 0.5×10^{-3} | 0.6×10^{-3} | 0.6×10^{-3} | 1.2×10^{-2} | 3.0×10^{-2} | 0.4×10^{-3} |
| Time res. p_T bins | 3.3×10^{-3} | 1.4×10^{-3} | 0.1×10^{-2} | $< 10^{-4}$ | $< 10^{-4}$ | 0.5×10^{-3} | 6.2×10^{-3} | 5.2×10^{-3} | 1.1×10^{-3} |
| Total | 1.8×10^{-2} | 0.2×10^{-2} | 0.1×10^{-2} | 0.2×10^{-2} | 0.4×10^{-2} | 0.4×10^{-2} | 9.7×10^{-2} | 2.0×10^{-1} | 0.1×10^{-1} |

Uncertainty in the calibration of the B_s -tag probability; MC statistical uncertainty included in fit stat. error

Alternative detector acceptance fit-functions and binning determined from MC

Radial expansion uncertainties determined from their effect on tracks d_0 in the data

Background angles model (fixed in UML fit) extracted from data with varying sidebands size and binning

Uncertainties of relative fraction; fit-model and P-wave contribution

Uncertainties of relative fraction; fit-model and contributions from $\Lambda b \rightarrow J/\psi \Lambda^*$ decays

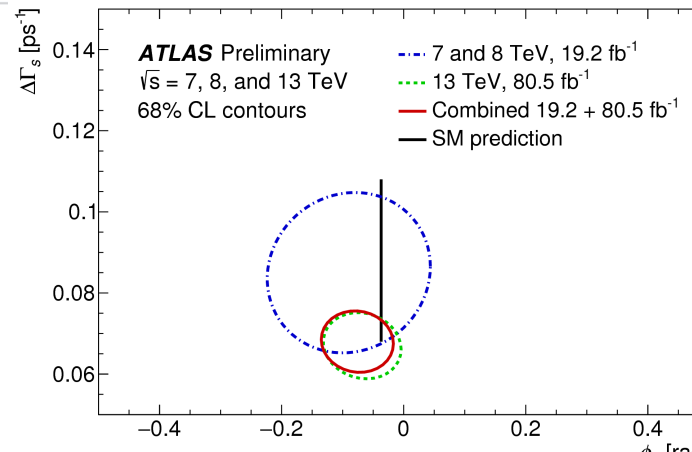
Toy-MC studies; pulls of the default fit model, default fit on toy-data generated with modified PDFs

Result of the CPV $B_s \rightarrow J/\psi \phi$ Study

| Parameter | Value | Statistical uncertainty | Systematic uncertainty |
|-----------------------------------|--------|-------------------------|------------------------|
| ϕ_s [rad] | -0.068 | 0.038 | 0.018 |
| $\Delta\Gamma_s$ [ps $^{-1}$] | 0.067 | 0.005 | 0.002 |
| Γ_s [ps $^{-1}$] | 0.669 | 0.001 | 0.001 |
| $ A_{ }(0) ^2$ | 0.219 | 0.002 | 0.002 |
| $ A_0(0) ^2$ | 0.517 | 0.001 | 0.004 |
| $ A_S(0) ^2$ | 0.046 | 0.003 | 0.004 |
| δ_{\perp} [rad] | 2.946 | 0.101 | 0.097 |
| $\delta_{ }$ [rad] | 3.267 | 0.082 | 0.201 |
| $\delta_{\perp} - \delta_S$ [rad] | -0.220 | 0.037 | 0.010 |

Fit correlation matrix:

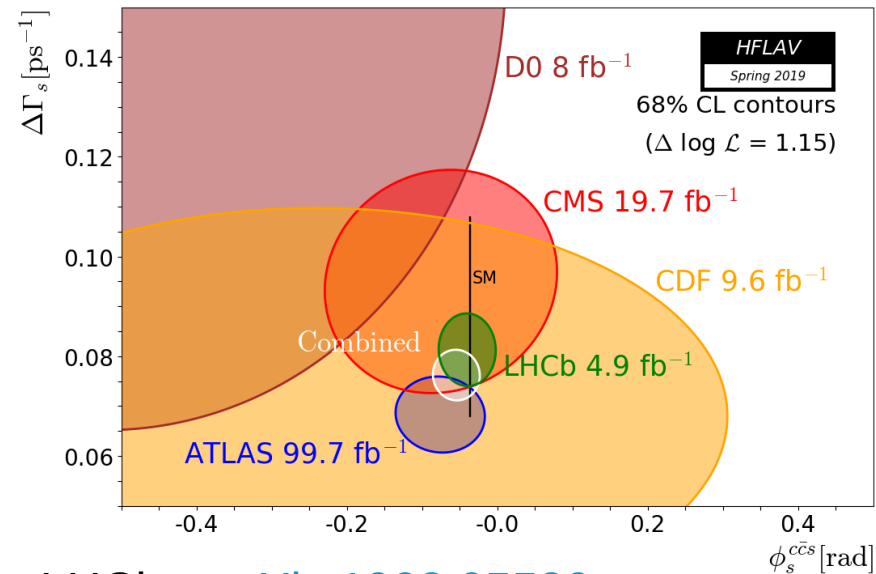
| | $\Delta\Gamma$ | Γ_s | $ A_{ }(0) ^2$ | $ A_0(0) ^2$ | $ A_S(0) ^2$ | $\delta_{ }$ | δ_{\perp} | $\delta_{\perp} - \delta_S$ |
|------------------|----------------|------------|-----------------|--------------|--------------|---------------|------------------|-----------------------------|
| ϕ_s | -0.111 | 0.038 | 0.000 | -0.008 | -0.015 | 0.019 | -0.001 | -0.011 |
| $\Delta\Gamma$ | 1 | -0.563 | 0.092 | 0.097 | 0.042 | 0.036 | 0.011 | 0.009 |
| Γ_s | | 1 | -0.139 | -0.040 | 0.103 | -0.105 | -0.041 | 0.016 |
| $ A_{ }(0) ^2$ | | | 1 | -0.349 | -0.216 | 0.571 | 0.223 | -0.035 |
| $ A_0(0) ^2$ | | | | 1 | 0.299 | -0.129 | -0.056 | 0.051 |
| $ A_S(0) ^2$ | | | | | 1 | -0.408 | -0.175 | 0.164 |
| $\delta_{ }$ | | | | | | 1 | 0.392 | -0.041 |
| δ_{\perp} | | | | | | | 1 | 0.052 |



Combination with 7 TeV and 8 TeV results

- We present a combined result (BLUE) of this result with our previous “run-1” result.

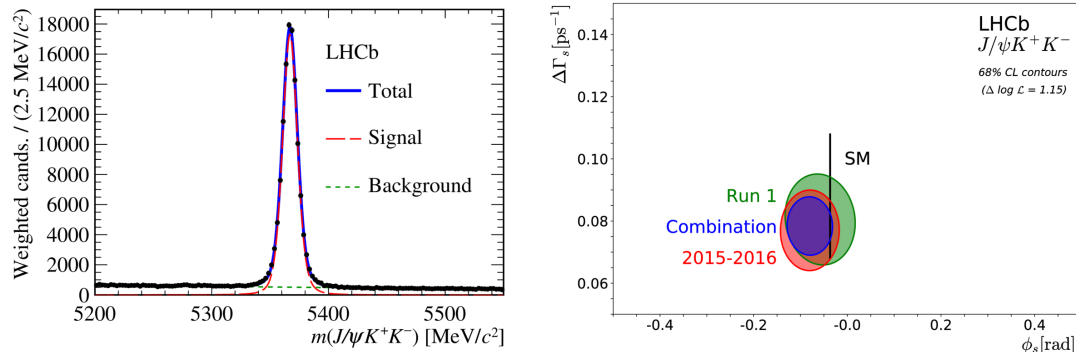
| Parameter | Value | Statistical uncertainty | Systematic uncertainty |
|-----------------------------------|--------|-------------------------|------------------------|
| ϕ_s [rad] | -0.076 | 0.034 | 0.019 |
| $\Delta\Gamma_s$ [ps $^{-1}$] | 0.068 | 0.004 | 0.003 |
| Γ_s [ps $^{-1}$] | 0.669 | 0.001 | 0.001 |
| $ A_{ }(0) ^2$ | 0.220 | 0.002 | 0.002 |
| $ A_0(0) ^2$ | 0.517 | 0.001 | 0.004 |
| $ A_S ^2$ | 0.043 | 0.004 | 0.004 |
| δ_{\perp} [rad] | 3.075 | 0.096 | 0.091 |
| $\delta_{ }$ [rad] | 3.295 | 0.079 | 0.202 |
| $\delta_{\perp} - \delta_S$ [rad] | -0.216 | 0.037 | 0.010 |



LHCb: [arXiv:1903.05530](https://arxiv.org/abs/1903.05530)
 ATLAS:
[ATLAS-CONF-2019-009](https://atlas-conference.cern.ch/2019/009.html)

LHCb - 2019

- LHCb have recently released an updated result.
- LHCb has particle ID hardware allowing them to significantly reduce background, but cannot record as much luminosity reducing statistics
- Resulting in a worse statistical error but better systematic error.



$$\Phi_s = -0.083 \pm 0.041 \pm 0.006 \text{ rad}$$

$$\Delta\Gamma_s = 0.077 \pm 0.008 \pm 0.003 \text{ ps}^{-1}$$

ATLAS

$$\begin{aligned} \phi_s &= -0.076 \pm 0.034 \text{ (stat.)} \pm 0.019 \text{ (syst.) rad} \\ \Delta\Gamma_s &= 0.068 \pm 0.004 \text{ (stat.)} \pm 0.003 \text{ (syst.) ps}^{-1} \end{aligned}$$

CMS - 2015

- CMS have a measurement from 2015 using run-1 data.
- CMS has a similar strategy to ATLAS but cut out the direct pp background.

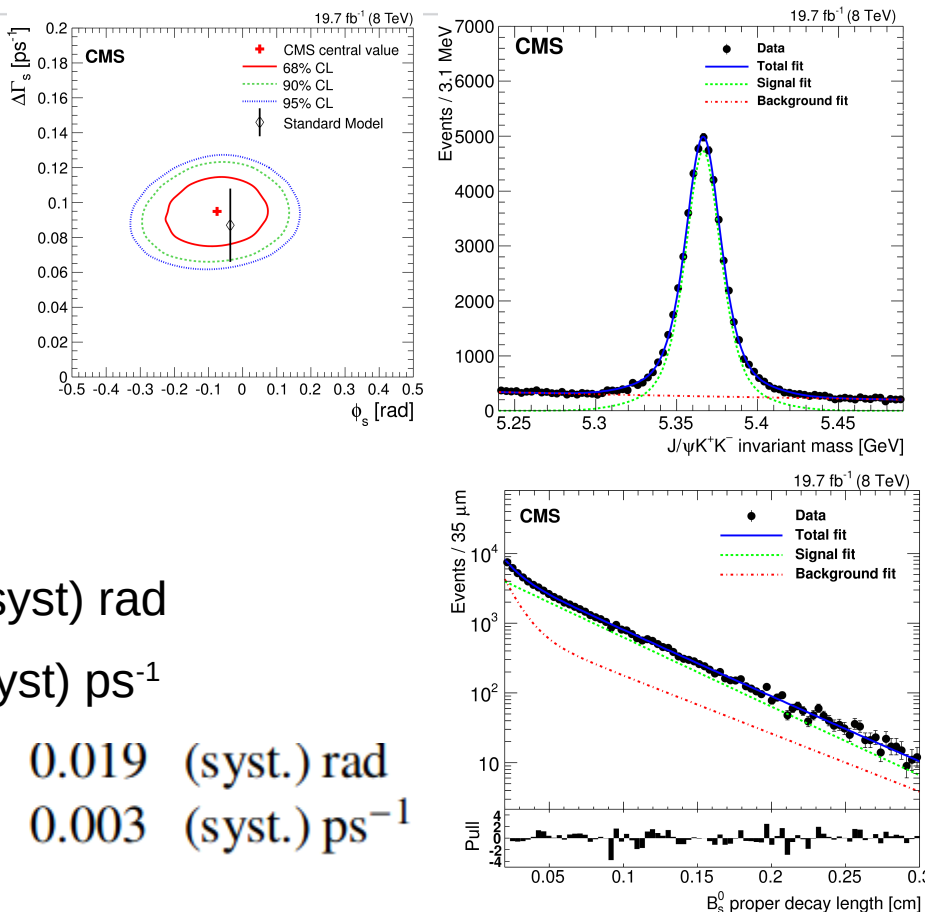
$$\phi_s = -0.075 \pm 0.097 \text{ (stat)} \pm 0.031 \text{ (syst) rad}$$

$$\Delta\Gamma_s = 0.095 \pm 0.013 \text{ (stat)} \pm 0.007 \text{ (syst) ps}^{-1}$$

CMS

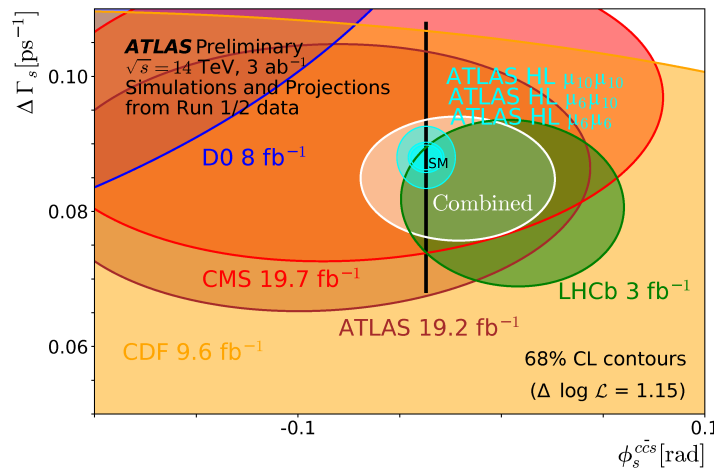
ATLAS

$$\begin{array}{lclclcl} \phi_s & = & -0.076 & \pm & 0.034 & \text{(stat.)} & \pm & 0.019 & \text{(syst.) rad} \\ \Delta\Gamma_s & = & 0.068 & \pm & 0.004 & \text{(stat.)} & \pm & 0.003 & \text{(syst.) ps}^{-1} \end{array}$$

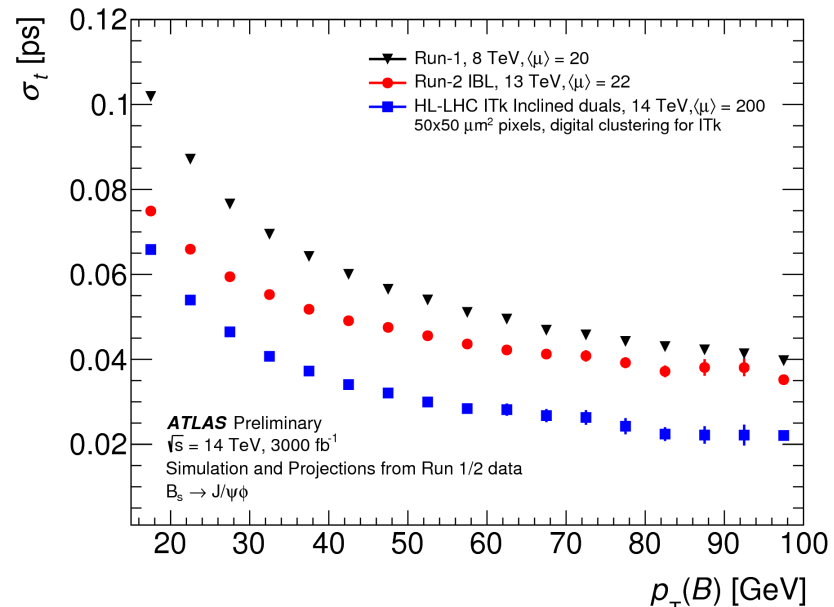


Detector Improvements

- In run-2 IBL improves time resolution → improved ϕ_s
- We estimate ϕ_s for future analyses give various muon threshold scenarios.



ATL-PHYS-PUB-2018-041



Summary

- ATLAS' measurement is compatible with the standard model and other experiments.
- ATLAS remains competitive with other experiments

| | | | | | | | |
|-----------------------------|---|--------|-------|---------------|-------|---------------|------------------|
| ϕ_s | = | -0.076 | \pm | 0.034 (stat.) | \pm | 0.019 (syst.) | rad |
| $\Delta\Gamma_s$ | = | 0.068 | \pm | 0.004 (stat.) | \pm | 0.003 (syst.) | ps^{-1} |
| Γ_s | = | 0.669 | \pm | 0.001 (stat.) | \pm | 0.001 (syst.) | ps^{-1} |
| $ A_{\parallel}(0) ^2$ | = | 0.220 | \pm | 0.002 (stat.) | \pm | 0.002 (syst.) | |
| $ A_0(0) ^2$ | = | 0.517 | \pm | 0.001 (stat.) | \pm | 0.004 (syst.) | |
| $ A_S(0) ^2$ | = | 0.043 | \pm | 0.004 (stat.) | \pm | 0.004 (syst.) | |
| δ_{\perp} | = | 3.075 | \pm | 0.096 (stat.) | \pm | 0.091 (syst.) | rad |
| δ_{\parallel} | = | 3.295 | \pm | 0.079 (stat.) | \pm | 0.202 (syst.) | rad |
| $\delta_{\perp} - \delta_S$ | = | -0.216 | \pm | 0.037 (stat.) | \pm | 0.010 (syst.) | rad |